

Supporting information

From Monomeric Tin(II) Hydride to Non-symmetric Distannyne

Miroslav Novák,^[b] Libor Dostál,^[a] Zdenka Růžicková,^[a] Stefan Mebs,^{[d]*} Jens Beckmann^{[c]*} and Roman Jambor^{[a]*}

[a] Department of General and Inorganic Chemistry, University of Pardubice, 532 10 Pardubice, Czech Republic
E-mail: roman.jambor@upce.cz,

[b] Institute of Chemistry and Technology of Macromolecular Materials, University of Pardubice, 532 10 Pardubice, Czech Republic

[c] Institut für Anorganische Chemie und Kristallographie, Universität Bremen, Leobener Straße 7, 28359 Bremen, Germany. E-Mail: j.beckmann@uni-bremen.de

[d] Institut für Experimentalphysik, Freie Universität Berlin, Arnimallee 14, 14195 Berlin, Germany. E-Mail: stebs@chemie.fu-berlin.de

Contents:

Experimental Section	pages S3 – S6
Table S1. Crystallographic data of compounds 2 and 4 ·(C ₆ H ₁₄) _{0.5} .	page S7
Table S2. Topological and integrated bond properties from AIM and ELI-D	page S8
Table S3. AIM atomic and fragmental charges (in e)	page S8
Figure S1. ¹ H NMR (C ₆ D ₆ , 500MHz) of L ² (Cl)Sn·W(CO) ₅ (1).	page S9
Figure S2. ¹³ C{ ¹ H} NMR (C ₆ D ₆ , 125 MHz) of L ² (Cl)Sn·W(CO) ₅ (1)	page S10
Figure S3. ¹¹⁹ Sn{ ¹ H} NMR (C ₆ D ₆ , 186 MHz) of L ² (Cl)Sn·W(CO) ₅ (1)	page S11
Figure S4. ¹ H NMR (C ₆ D ₆ , 500MHz) of L ² (H)Sn·W(CO) ₅ (2)	page S12
Figure S5. ¹³ C{ ¹ H} NMR (C ₆ D ₆ , 125 MHz) of L ² (H)Sn·W(CO) ₅ (2)	page S13
Figure S6. ¹¹⁹ Sn{ ¹ H} NMR (C ₆ D ₆ , 186 MHz) of L ² (H)Sn·W(CO) ₅ (2)	page S14
Figure S7. ¹ H NMR (C ₆ D ₆ , 500MHz) of L ¹ SnNEt ₂ (3).	page S15
Figure S8. ¹³ C{ ¹ H} APT NMR (C ₆ D ₆ , 125 MHz) of L ¹ SnNEt ₂ (3)	page S16
Figure S9. ¹¹⁹ Sn{ ¹ H} NMR (C ₆ D ₆ , 186 MHz) L ¹ SnNEt ₂ (3)	page S17
Figure S10. ¹ H NMR spectrum of L ² Sn·W(CO) ₅ -SnL ¹ ·(C ₆ H ₁₄) _{0.5} (4 ·(C ₆ H ₁₄) _{0.5})	page S18
Figure S11. ¹³ C{ ¹ H} APT NMR (C ₆ D ₆ , 125 MHz) of L ² Sn·W(CO) ₅ -SnL ¹ ·(C ₆ H ₁₄) _{0.5} (4 ·(C ₆ H ₁₄) _{0.5})	page S19
Figure S12. ¹¹⁹ Sn{ ¹ H} NMR (C ₆ D ₆ , 186 MHz) of L ² Sn·W(CO) ₅ -SnL ¹ ·(C ₆ H ₁₄) _{0.5} (4 ·(C ₆ H ₁₄) _{0.5})	page S20
Figure S13. RSBI analysis of 2 . (a) AIM bond paths motif, (b) NCI <i>iso</i> -surface at s(r) = 0.5, (c) ELI-D localization domain representation at <i>iso</i> -value of 1.2, (d) ELI-D distribution mapped on the Sn–W ELI-D basin.	page S21

Experimental Section

General Methods. All moisture and air sensitive reactions were carried out under an argon atmosphere using standard Schlenk tube techniques. All solvents were dried using Pure Solv–Innovative Technology equipment. Starting compounds $L^1(Cl)Sn$ and $L^2(Cl)Sn$ were prepared according to literature procedures.¹ $W(CO)_6$, $K[(Et)_3BH]$, Et_2NH and $nBuLi$ (1.6M in hexane) were purchased from Sigma Aldrich and used as received. Elemental analyses were performed on an LECO-CHNS-932 analyser. Melting points were measured with a Stuart melting-point apparatus. Solid state IR spectra were recorded on a Nicolet 6700 FTIR spectrometer using single-bounce silicon ATR crystal (resolution 2 cm^{-1}). The 1H , $^{13}C\{^1H\}$ and $^{119}Sn\{^1H\}$ NMR spectra were recorded on Bruker 500 NMR spectrometer at 298 K in C_6D_6 . The 1H and $^{13}C\{^1H\}$ NMR spectra were referenced internally to residual protio-solvent and solvent resonances, respectively, and are reported relative to Me_4Si ($\delta = 0$ ppm). The $^{119}Sn\{^1H\}$ NMR spectra were referenced externally to Me_4Sn ($\delta = 0$ ppm). Compounds **1** – **4** were characterized by the help of NMR spectroscopy, elemental analysis (except of **4**) and X-ray diffraction analysis for **2** and **4**.

Synthesis.

$L^2(Cl)Sn \cdot W(CO)_5$ (**1**). Solution of $W(CO)_6$ (0.67 g, 3.05 mmol) in THF (200 mL) was UV-irradiated ($\lambda = 254$ nm) at room temperature for 1 hour. The resulting orange solution of $W(CO)_5 \cdot THF$ was added dropwise to a stirred solution of $L^2(Cl)Sn$ (1.31 g, 3.05 mmol) in THF (10 mL). The mixture was stirred overnight. After that, all volatiles were removed under reduced pressure, the residue was suspended in toluene (20 mL) and the insoluble material was filtered off. The toluene filtrate was evaporated and the solid was washed with cold hexane (5 mL) to afford yellow powder material characterized as **1**. Yield: 1.40 g (74 %); Mp: 150-152 °C; Anal. Calc. for $C_{24}H_{32}ClNO_5SnW$ (752.52): C, 38.31; H, 4.29. Found: C, 38.6; H, 4.5. 1H NMR (C_6D_6 , 500 MHz): δ 0.49 (t, 3H, $J_{HH} = 7.0$ Hz), 0.62 (t, 3H, $J_{HH} = 7.0$ Hz), 1.27 (s, 9H), 1.54 (s, 9H), 2.25 (m, 1H), 2.47 (m, 1H), 2.85 (m, 1H), 2.99 (m, 1H), 3.20 (d, AX system, 1H, $J_{HH} = 14.9$ Hz, CH_2N), 3.83 (d, AX system, 1H, $J_{HH} = 14.9$ Hz, CH_2N), 6.86 (s, 1H), 7.53 (s, 1H). $^{13}C\{^1H\}$ NMR (C_6D_6 , 125.77 MHz): δ 8.7, 9.9, 31.1, 33.3, 34.8, 37.3, 46.6, 48.1, 60.3, 120.4, 123.1, 143.2, 150.2, 152.6, 158.0, 198.2 ($J_{CSn} = 49$ Hz, $J_{CW} = 123$ Hz), 199.4 ($J_{CW} = 154$ Hz). $^{119}Sn\{^1H\}$ NMR (C_6D_6 , 186.49 MHz): δ 270.7 ($J_{SnW} = 1160$ Hz). FT-IR (ATR, cm^{-1}): 2064, 1976, 1930, 1900 (CO).

$L^2(H)Sn\cdot W(CO)_5$ (**2**). THF solution of $K[(Et)_3BH]$ (0.36 mL, 1M) was added dropwise to a stirred solution of **1** (0.28 g, 0.36 mmol) in THF (15 mL) at $-20\text{ }^\circ\text{C}$ and the mixture was stirred for 1 hour at this temperature. After that, all volatiles were removed under reduced pressure, the residue was suspended in hexane (20 mL) and the insoluble material was filtered off. The hexane filtrate was concentrated and cooled to $-20\text{ }^\circ\text{C}$ to afford pale yellow crystalline material characterized as **2**. Yield: 0.33 g (62 %). Mp: $87\text{--}88\text{ }^\circ\text{C}$; Anal. Calc. for $C_{24}H_{33}NO_5SnW$ (718.07): C, 40.14; H, 4.63. Found: C, 40.3; H, 4.7. 1H NMR (C_6D_6 , 500 MHz): δ 0.28 (t, 3H, $J_{HH} = 7.8$ Hz), 0.72 (t, 3H, $J_{HH} = 7.8$ Hz), 1.28 (s, 9H), 1.41 (s, 9H), 2.37 (m, 2H), 2.43 (m, 1H), 2.80 (m, 1H), 3.18 (d, AX system, 1H, $J_{HH} = 14.0$ Hz, CH_2N), 3.52 (d, AX system, 1H, $J_{HH} = 14.0$ Hz, CH_2N), 6.90 (s, 1H), 7.55 (s, 1H), 10.25 (s, 1H, $J_{HSn} = 1091$ Hz, $J_{HW} = 15.6$ Hz, Sn-H). $^{13}C\{^1H\}$ NMR (C_6D_6 , 125.77 MHz): δ 8.2, 12.1, 32.0, 32.5, 35.3, 37.8, 46.5, 48.6, 61.7, 121.6, 124.2, 142.0, 144.3, 152.0, 159.2, 200.7 ($J_{CW} = 122$ Hz, $J_{CSn} = 50$ Hz), 202.4 ($J_{CW} = 160$ Hz, $J_{CSn} = 38$ Hz). $^{119}Sn\{^1H\}$ NMR (C_6D_6 , 186.49 MHz): δ 268.6 ($J_{SnW} = 942$ Hz). FT-IR (ATR, cm^{-1}): 2056, 1937, 1915, 1989 (CO), 1781 (Sn-H).

L^1SnNEt_2 (**3**). Hexane solution of $nBuLi$ (0.82 mL, 1.6M) was added to a stirred solution of Et_2NH (96 mg, 1.31 mL) in hexane (10 mL) at $0\text{ }^\circ\text{C}$. The resulting white suspension was stirred at this temperature for 30 min and then added dropwise to a stirred solution of $L^1(Cl)Sn$ (0.45 g, 1.31 mmol) in toluene (20 mL) pre-cooled to $-78\text{ }^\circ\text{C}$. The reaction mixture was left to warm-up and stirred for 30 min. After that, all volatiles were removed under reduced pressure, the residue was suspended in hexane (20 mL) and the insoluble material was filtered off. The evaporation of hexane filtrate afforded pale yellow oil characterized as **3**. Yield: 0.41 g (82 %). Anal. Calc. for $C_{16}H_{29}N_3Sn$ (382.13): C, 50.29; H, 7.65. Found: C, 50.0, H, 7.6. 1H NMR (C_6D_6 , 500 MHz): δ 1.30 (t, 6H, $J_{HH} = 6.9$ Hz), 2.30 (br, 12H), 3.42 (d, AX system, 2H, $J_{HH} = 13.2$ Hz, CH_2N), 3.54 (br, 4H), 3.65 (d, AX system, 2H, $J_{HH} = 13.2$ Hz, CH_2N), 7.10 (d, 2H, $J_{HH} = 7.4$ Hz), 7.26 (t, 1H, $J_{HH} = 7.4$ Hz). $^{13}C\{^1H\}$ NMR (C_6D_6 , 125.77 MHz): δ 19.0, 46.1, 47.5, 67.0, 125.2, 127.8, 147.6, 170.5. $^{119}Sn\{^1H\}$ NMR (C_6D_6 , 186.49 MHz): δ 193.9.

$L^2Sn\cdot W(CO)_5\cdot SnL^1$ (**4**). Solution of **2** (0.20 g, 0.53 mmol) in freshly degassed toluene (10 mL) was added dropwise to a stirred solution of **3** (0.38 g, 0.53 mmol) in freshly degassed toluene (10 mL) at room temperature. The reaction mixture was stirred for 5 hours and the colour of mixture changed from yellow to orange. After that, all volatiles were removed under reduced pressure, the residue was suspended in hexane (20 mL) and the insoluble material was filtered off. The hexane filtrate was concentrated and cooled to $4\text{ }^\circ\text{C}$ to afford orange crystalline

material characterized as $4 \cdot (\text{C}_6\text{H}_{14})_{0.5}$. Yield: 0.34 g (62 %). Mp: 170-174 °C (with decomp.); Anal. Calc. for $\text{C}_{42}\text{H}_{65}\text{N}_3\text{O}_5\text{Sn}_2\text{W}$ (1113.24): C, 45.31; H, 5.89. Found: C, 46.8; H, 6.0. All attempts to get satisfied data for elemental analysis failed due to high reactivity of **4**. ^1H NMR (C_6D_6 , 500.13 MHz) δ 0.63 (t, 3H, $J_{\text{HH}} = 7.8$ Hz), 1.26 (s, 9H), 1.28 (s, 9H), 1.90 (s, 6H), 2.17 (s, 6H), 2.59 (m, 2H), 3.07 (m, 1H), 3.08 (d, AX system, 1H, $J_{\text{HH}} = 13.5$ Hz, CH_2N), 3.15 (d, AX system, 1H, $J_{\text{HH}} = 13.5$ Hz, CH_2N), 3.41 (d, AX system, 1H, $J_{\text{HH}} = 13.5$ Hz, CH_2N), 3.49 (d, AX system, 1H, $J_{\text{HH}} = 13.5$ Hz, CH_2N), 3.80 (d, AX system, 1H, $J_{\text{HH}} = 13.5$ Hz, CH_2N), 3.82 (d, AX system, 1H, $J_{\text{HH}} = 13.5$ Hz, CH_2N), 6.87 (t, 2H, $J_{\text{HH}} = 6.6$ Hz), 6.92 (s, 1H), 7.05 (t, 1H, $J_{\text{HH}} = 6.6$ Hz), 7.43 (s, 1H). $^{13}\text{C}\{^1\text{H}\}$ NMR (C_6D_6 , 125.77 MHz): δ 8.9, 12.8, 32.1, 32.5, 33.0, 35.0, 46.5, 47.2, 47.8, 47.9, 62.8, 68.5, 69.1, 121.1, 124.4, 125.0, 125.4, 127.8, 141.6, 146.6, 146.7, 149.8, 153.1, 159.1, 170.5, 200.7 ($J_{\text{CW}} = 126$ Hz), 205.7 ($J_{\text{CW}} = 122$ Hz). $^{119}\text{Sn}\{^1\text{H}\}$ NMR (C_6D_6 , 186.49 MHz): δ 396.8 (Sn \rightarrow W), 608.7. FT-IR (ATR, cm^{-1}): 2037, 1966, 1954, 1897 (CO).

Crystallography. The X-ray data for crystals of **2** and **4** were obtained at 150K using Oxford Cryostream low-temperature device on a Nonius KappaCCD diffractometer with Mo/ $\text{K}\alpha$ radiation ($\lambda = 0.71073$ Å), a graphite monochromator, and the ϕ and χ scan mode. Crystals of **2** and **4** were obtained from hexane solutions of the parent compounds at 4 °C. Data reductions were performed with DENZO-SMN.² The absorption was corrected by integration methods.³ Structures were solved by direct methods (Sir92)⁴ and refined by full matrix least-square based on F^2 (SHELXL97).⁵ Hydrogen atoms were mostly localized on a difference Fourier map, however to ensure uniformity of treatment of crystal, all hydrogen were recalculated into idealized positions (riding model) and assigned temperature factors $\text{H}_{\text{iso}}(\text{H}) = 1.2 U_{\text{eq}}$ (pivot atom) or of $1.5U_{\text{eq}}$ (methyl). H atoms in methyl, methylene moieties and hydrogen atoms in aromatic rings were placed with C-H distances of 0.96, 0.97 and 0.93 Å. The hydrogen atom of the Sn-H moiety was placed according the Fourier difference electron density map. The solvent accessible void has been detected in the structure of **4**. As modeled by the PLATON/SQUEEZE procedure⁶, the void of 198 Å is able to accommodate one molecule of hexane per unit cell. $R_{\text{int}} = \sum |F_o^2 - F_{o,\text{mean}}^2| / \sum F_o^2$, $S = [\sum (w(F_o^2 - F_c^2)^2) / (N_{\text{diffs}} - N_{\text{params}})]^{1/2}$ for all data, $R(F) = \sum ||F_o| - |F_c|| / \sum |F_o|$ for observed data, $wR(F^2) = [\sum (w(F_o^2 - F_c^2)^2) / (\sum w(F_o^2)^2)]^{1/2}$ for all data. Crystallographic data for structural analysis have been deposited with the Cambridge Crystallographic Data Centre, CCDC nos. 1895317 and 1895318 for **2** and **4**. Copies of this information may be obtained free of charge from The

Director, CCDC, 12 Union Road, Cambridge CB2 1EY, UK (fax: +44-1223-336033; e-mail: deposit@ccdc.cam.ac.uk or www: <http://www.ccdc.cam.ac.uk>).

Computational Methodology. For the solid-state molecular geometries of **2** and **4**, density functional theory (DFT) computations were performed at the B3PW91/6-311+G(2df,p)⁷ level of theory using Gaussian09.⁸ C-H distances were extended to match listed values for neutron diffraction data.⁹ For the W and Sn atoms, effective core potentials (W: ECP60MDF, Sn: ECP28MDF)¹⁰ and corresponding cc-pVTZ basis sets¹⁰ were utilized. The wavefunction files were used for a topological analysis of the electron density according to the Atoms-In-Molecules space-partitioning scheme¹¹ using AIM2000,¹² whereas DGRID¹³ was used to generate and analyze the Electron-Localizability-Indicator (ELI-D) related real-space bonding descriptors¹⁴ applying a grid step size of 0.05 a.u. (0.12 a.u. for visualization). The NCI¹⁵ grids were computed with NCIPLOT (0.1 a.u. grids).¹⁶ Bond paths are displayed with AIM2000, while ELI-D and NCI figures are displayed with Molliso.¹⁷

Table S1. Crystallographic data of compounds **2** and **4**·(C₆H₁₄)_{0.5}.

	2	4 ·(C ₆ H ₁₄) _{0.5}
Empirical formula	C ₂₄ H ₃₃ NO ₅ SnW	C ₃₆ H ₅₁ N ₃ O ₅ Sn ₂ W·(C ₆ H ₁₄) _{0.5}
Colour	Light Yellow	Orange
Formula mass [g mol ⁻¹]	718.05	1070.11
Crystal system	Triclinic	Triclinic
Space group	P-1	P-1
<i>a</i> [Å]	10.5731(7)	10.2659(10)
<i>b</i> [Å]	11.8679(10)	10.8110(7)
<i>c</i> [Å]	12.3310(6)	19.2601(17)
α [°]	111.850(6)	84.700(5)
β [°]	93.933(4)	80.761(7)
γ [°]	109.114(7)	86.030(6)
<i>Z</i>	2	2
μ [mm ⁻¹]	5.313	3.959
<i>D_x</i> [Mg m ⁻³]	1.800	1.694
Crystal size [mm]	0.39x0.33x0.25	0.171x0.158x0.145
Crystal shape	Block	Block
θ range [°]	2.67-27.50	2.100-27.499
T _{min} /T _{max}	0.291/0.420	0.584/0.675
ρ max/min, e/Å ³	2.473/-2.307	0.713/-1.129
no. of reflections measured	25614	39604
no. of unique reflections; <i>R</i> _{int} ^[a]	6054; 0.0317	9452; 0.0328
no. of observed refs [<i>I</i> >2 σ (<i>I</i>)]	5545	8244
no. of parameters	289	424
<i>S</i> ^[b] all data	1.139	1.109
Final <i>R</i> ^[c] [<i>I</i> >2 σ (<i>I</i>)]	0.0305	0.0286
<i>wR</i> ^[c] (all data)	0.0792	0.0618

Table S2. Topological and integrated bond properties from AIM and ELI-D

model	contact or basin	d [Å]	$\rho(r)$ [eÅ ⁻³]	$\nabla^2\rho(r)$ [eÅ ⁻⁵]	G/ $\rho(r)$ [a.u.]	H/ $\rho(r)$ [a.u.]	N _{ELI} [e]	V _{ELI} [Å ³]	γ_{ELI}	RJI [%]
2	Sn–W	2.769	0.36	1.5	0.58	-0.28	2.21	14.8	1.23	79.1
4	Sn(1)–W	2.864	0.32	1.0	0.49	-0.27	1.88	12.0	1.23	75.3
4	Sn(1)–Sn(2)	2.998	0.30	-0.1	0.22	-0.25	2.16	16.8	1.38	67.1
2	Sn–N	2.292	0.46	4.4	0.89	-0.22	2.11	4.3	1.83	94.4
4	Sn(1)–N	2.364	0.40	3.6	0.82	-0.18	2.11	4.4	1.84	95.2
4	Sn(2)–N(2)	2.439	0.20	1.5	0.60	-0.06	2.11	4.4	1.86	96.6
4	Sn(2)–N(1)	2.724	0.34	3.0	0.76	-0.15	2.16	5.5	1.92	99.0
2	Sn–C	2.164	0.69	2.9	0.71	-0.42	2.26	8.7	1.77	78.2
4	Sn(2)–C	2.186	0.66	3.1	0.73	-0.40	2.30	8.3	1.80	80.5
4	Sn(1)–C	2.204	0.64	2.6	0.68	-0.40	2.24	8.5	1.78	79.0
2	Sn–H	1.742	0.72	2.1	0.67	-0.46	1.96	16.6	9.61	69.3
2	Sn···H	2.686	0.10	1.0	0.64	0.07				
4	Sn(1)···H	2.661	0.10	0.9	0.60	0.04				
4	Sn(2)···H	2.876	0.07	0.5	0.49	0.05				
4	LP(Sn(2))						2.11	23.3	1.97	98.0

For all bonds, $\rho(\mathbf{r})_{\text{bcp}}$ is the electron density at the bond critical point, $\nabla^2\rho(\mathbf{r})_{\text{bcp}}$ is the corresponding Laplacian, $G/\rho(\mathbf{r})_{\text{bcp}}$ and $H/\rho(\mathbf{r})_{\text{bcp}}$ are the kinetic and total energy density over $\rho(\mathbf{r})_{\text{bcp}}$ ratios, N_{ELI} and V_{ELI} are electron populations and volumes of related ELI-D basins, γ_{ELI} is the ELI-D value at the attractor position, RJI is the Raub-Jansen-Index, no. refers to the number of averaged bonds.

Table S3. AIM atomic and fragmental charges (in e)

2	Q _{tot}	4	Q _{tot}
CO [§]	-0.35	CO [§]	-0.39
W	1.39	W	1.40
L ²	-0.27	L ²	-0.35
(Sn)H	-0.38	L ¹	-0.37
Sn	1.03	Sn(1)	0.58
		Sn(2)	0.69
SUM	0.00	SUM	0.01

L² = 2-Et₂NCH₂-4,6-tBu₂-C₆H₂, L¹ = 2,6-(Me₂NCH₂)₂C₆H₃; § averaged value

Figure S1. ^1H NMR (C_6D_6 , 500MHz) of $\text{L}^2(\text{Cl})\text{Sn}\cdot\text{W}(\text{CO})_5$ (**1**).

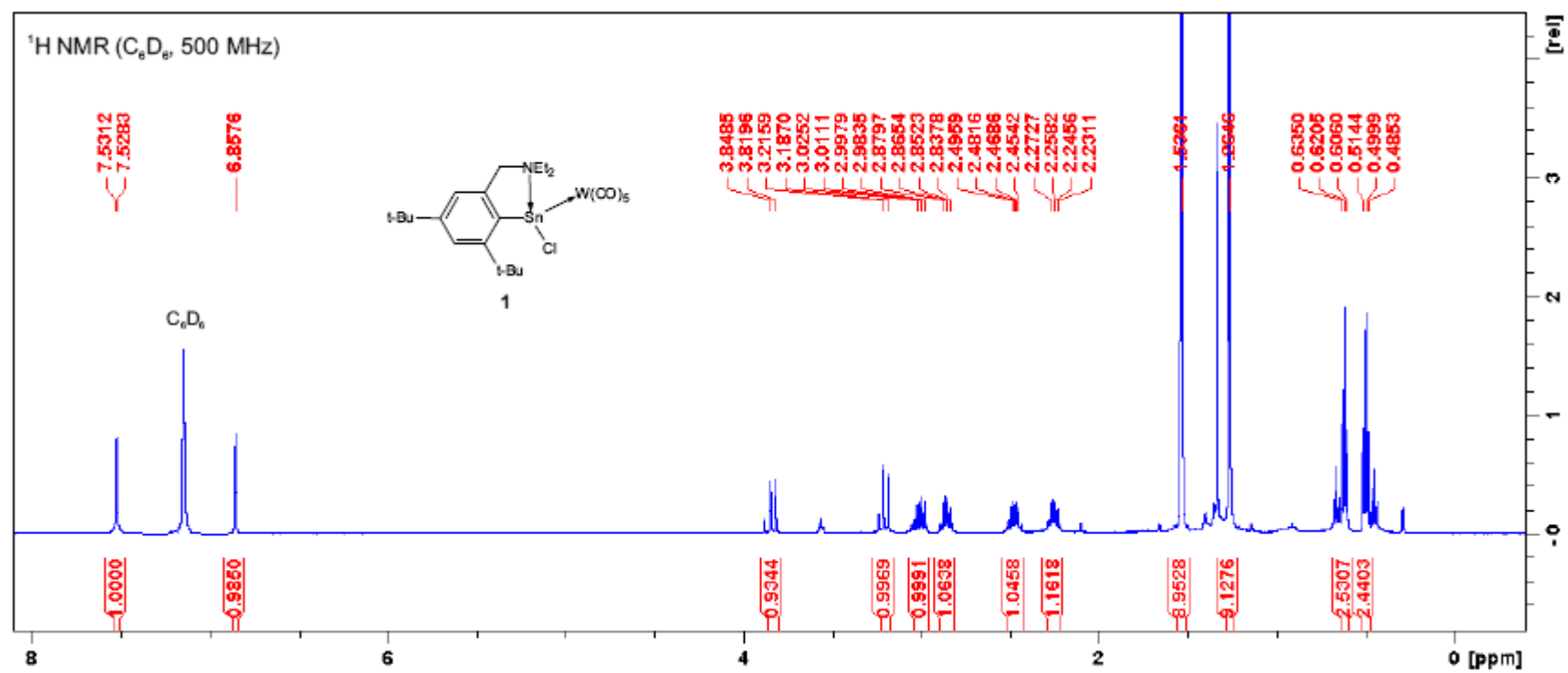


Figure S2. $^{13}\text{C}\{^1\text{H}\}$ NMR (C_6D_6 , 125 MHz) of $\text{L}^2(\text{Cl})\text{Sn}\cdot\text{W}(\text{CO})_5$ (**1**)

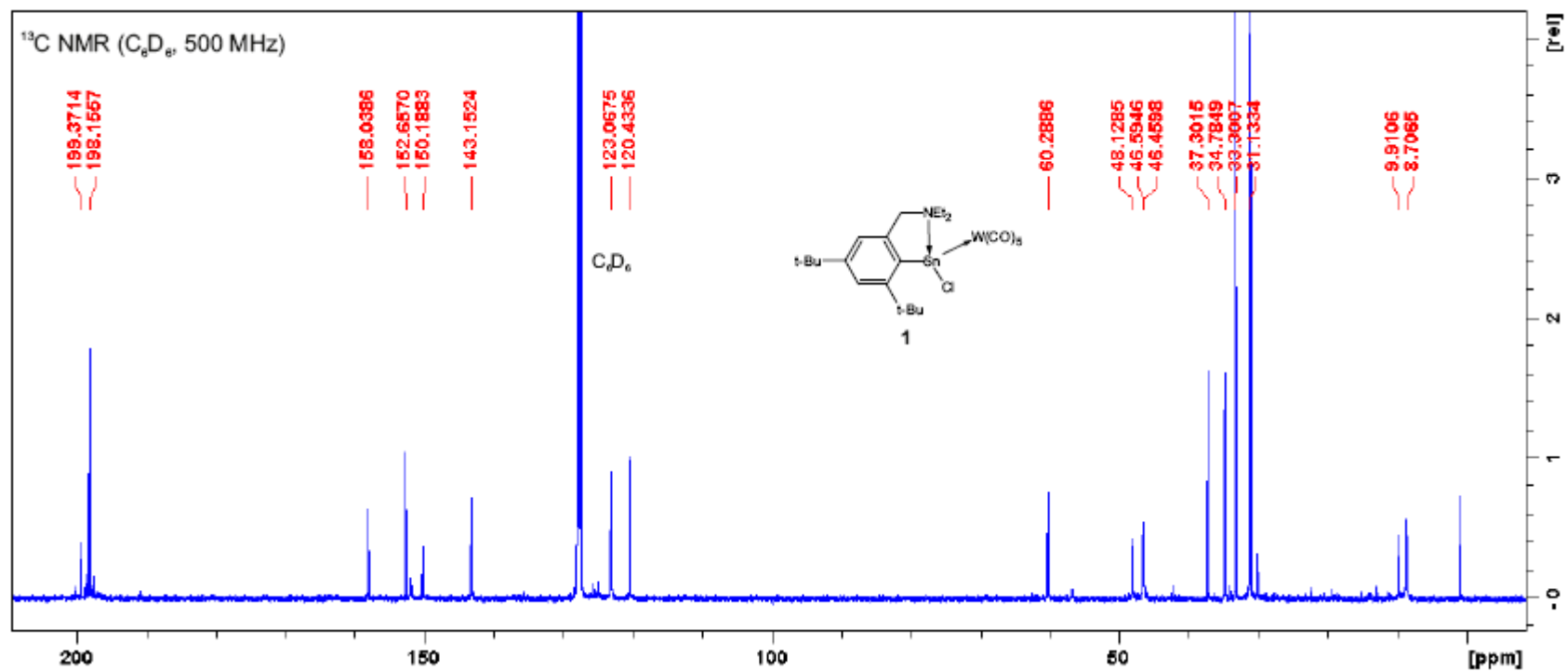


Figure S3. $^{119}\text{Sn}\{^1\text{H}\}$ NMR (C_6D_6 , 186 MHz) of $\text{L}^2(\text{Cl})\text{Sn}\cdot\text{W}(\text{CO})_5$ (**1**)

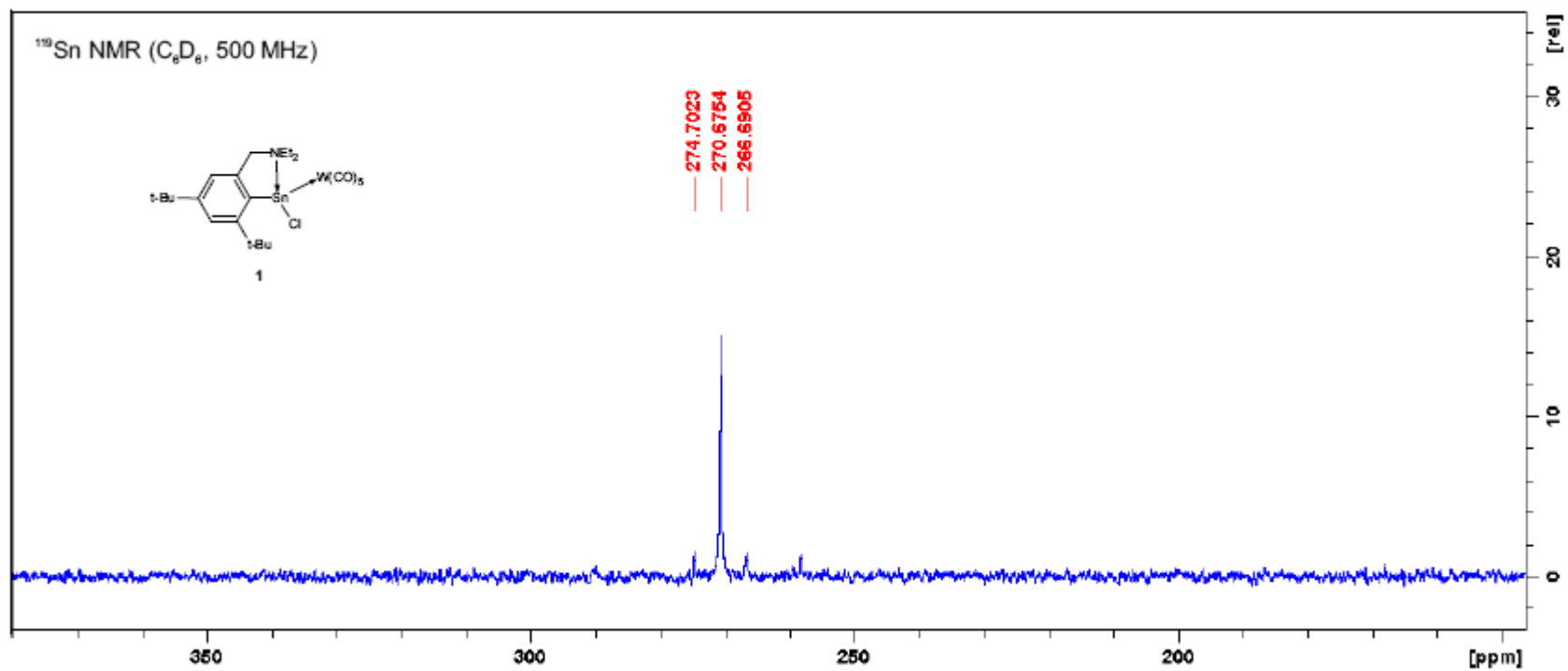


Figure S4. ^1H NMR (C_6D_6 , 500MHz) of $\text{L}^2(\text{H})\text{Sn}\cdot\text{W}(\text{CO})_5$ (**2**)

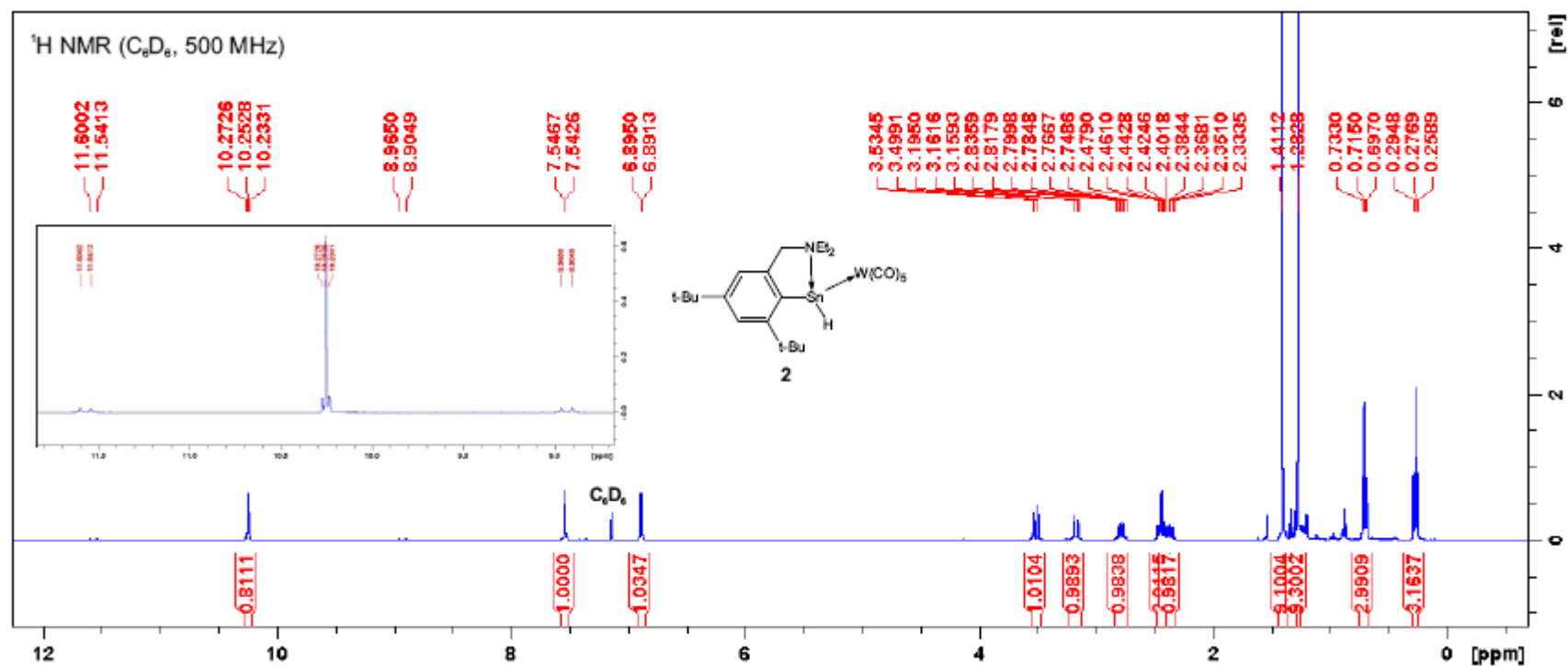


Figure S5. $^{13}\text{C}\{^1\text{H}\}$ NMR (C_6D_6 , 125 MHz) of $\text{L}^2(\text{H})\text{Sn}\cdot\text{W}(\text{CO})_5$ (**2**)

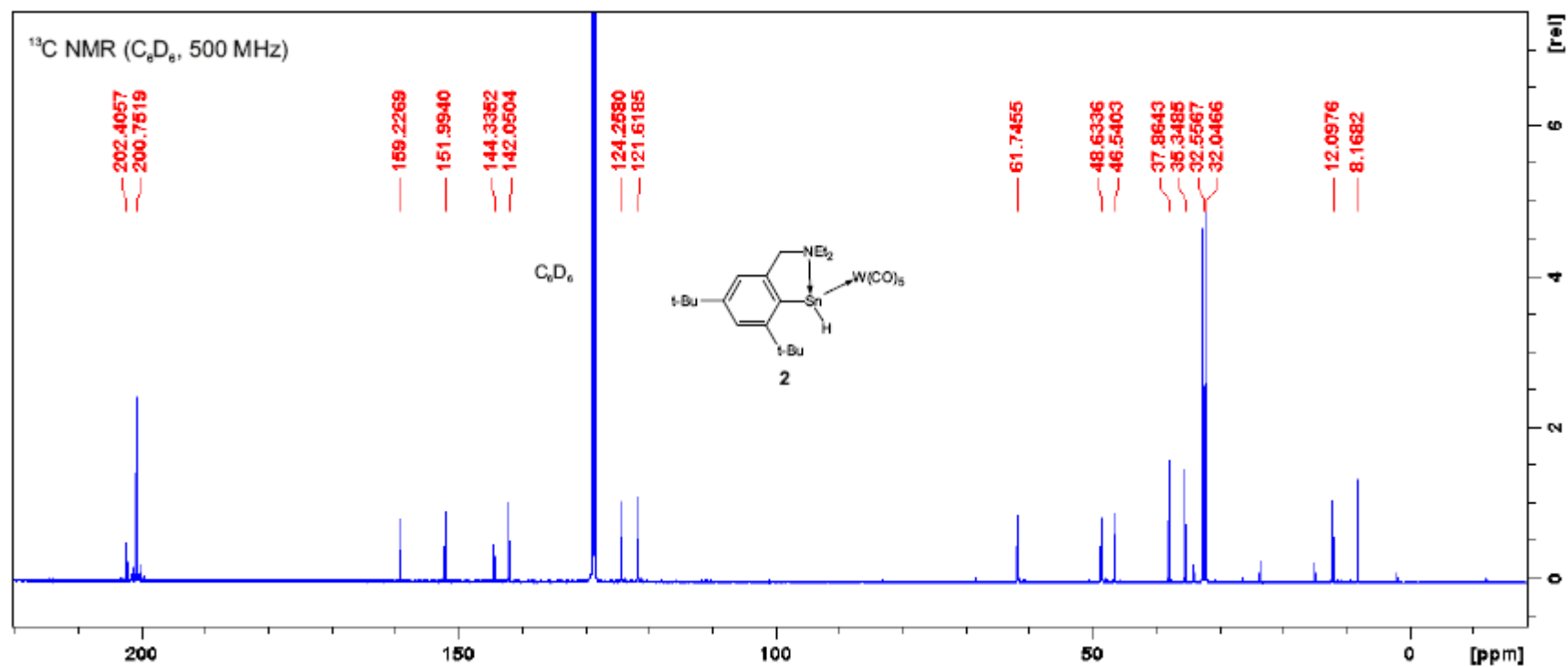


Figure S6. $^{119}\text{Sn}\{^1\text{H}\}$ NMR (C_6D_6 , 186 MHz) of $\text{L}^2(\text{H})\text{Sn}\cdot\text{W}(\text{CO})_5$ (**2**)

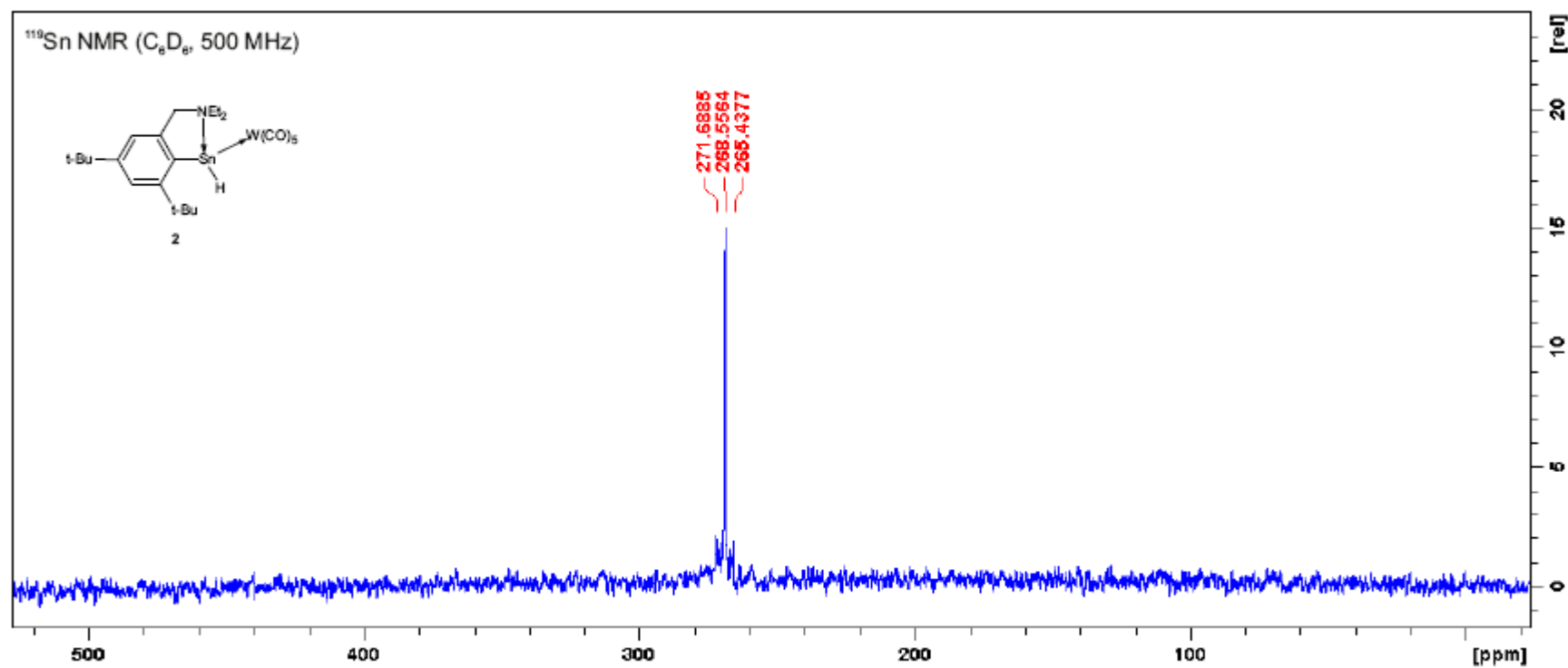


Figure S7. ^1H NMR (C_6D_6 , 500MHz) of L^1SnNEt_2 (**3**).

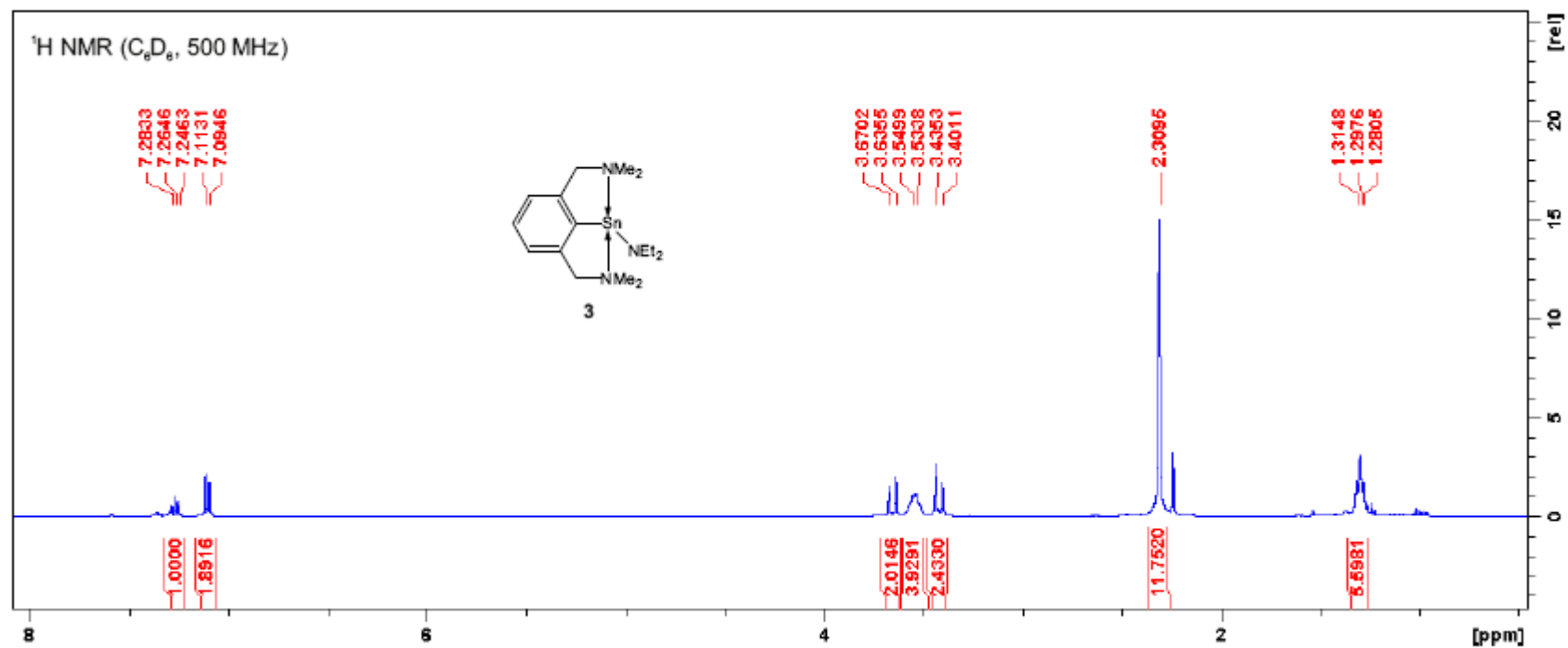


Figure S8. $^{13}\text{C}\{^1\text{H}\}$ APT NMR (C_6D_6 , 125 MHz) of L^1SnNEt_2 (**3**)

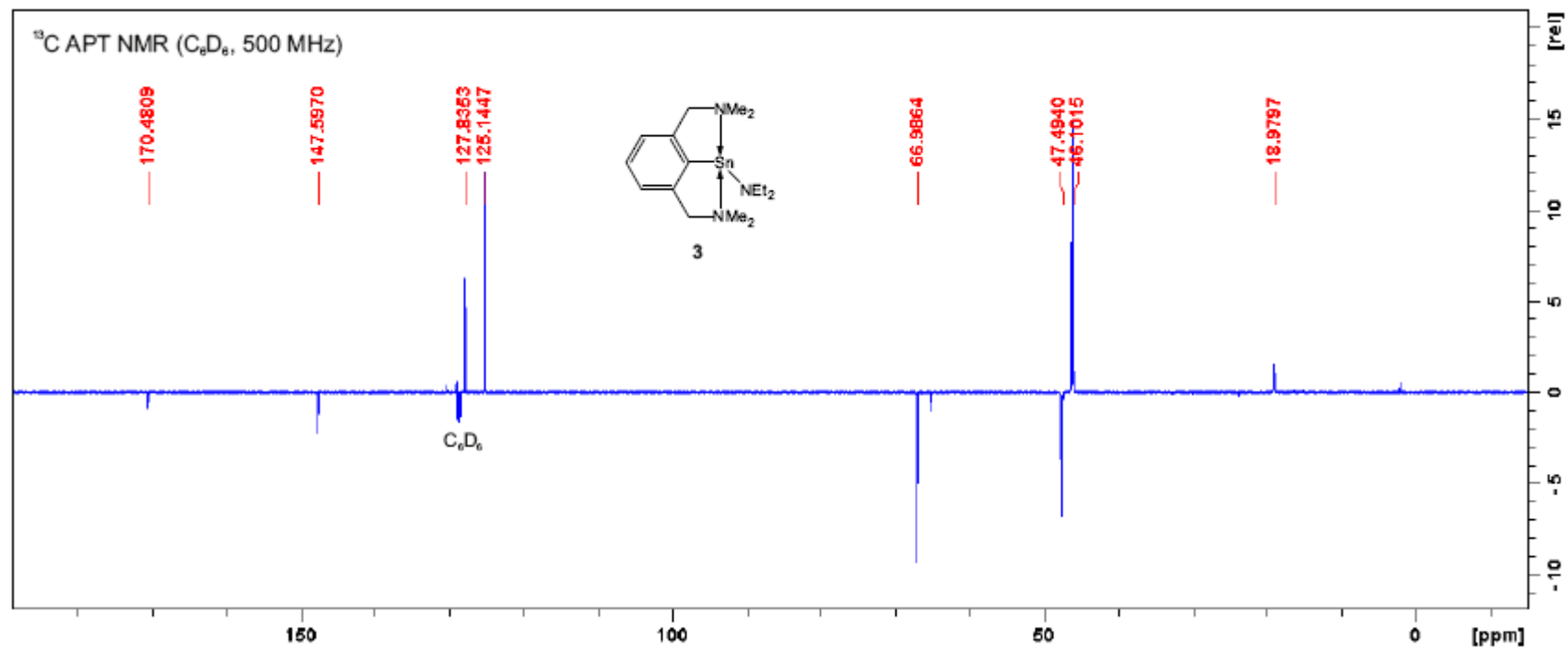


Figure S9. $^{119}\text{Sn}\{^1\text{H}\}$ NMR (C_6D_6 , 186 MHz) L^1SnNEt_2 (**3**)

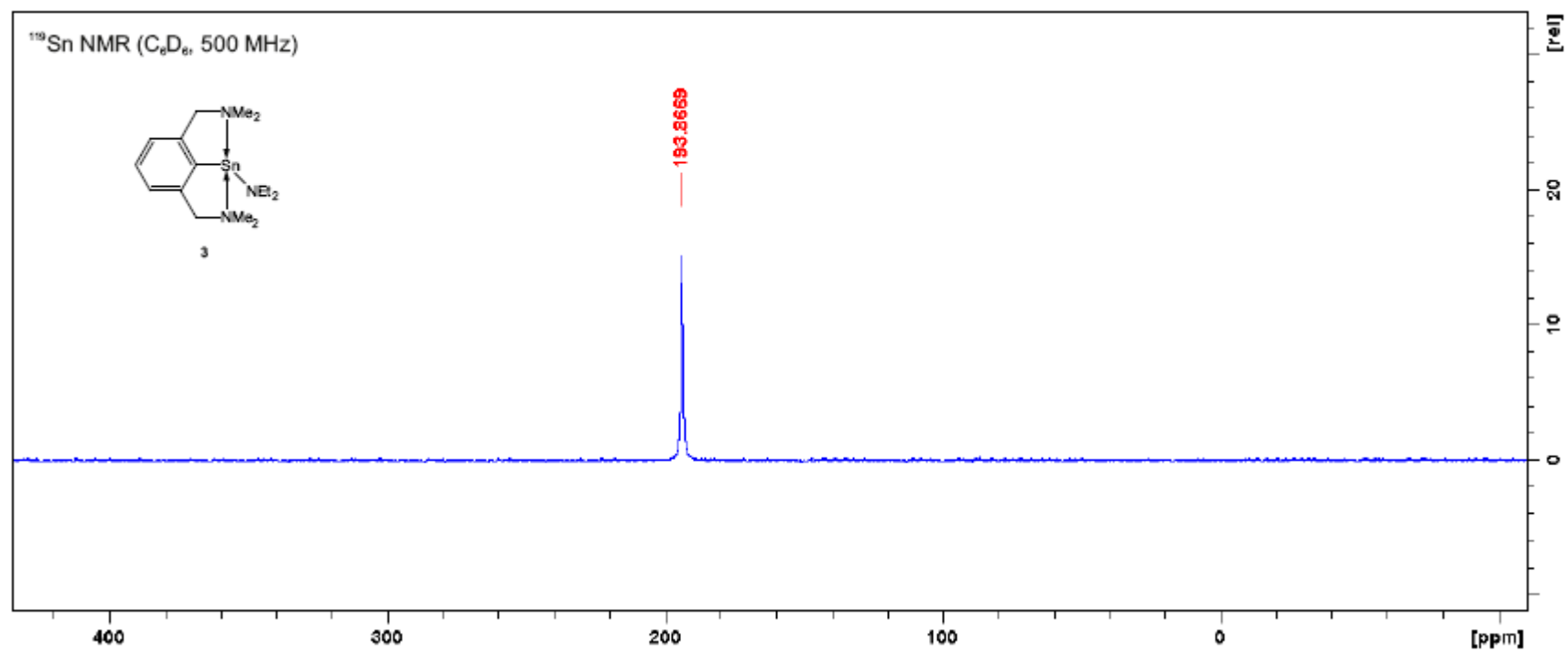


Figure S10. ^1H NMR spectrum of $\text{L}^2\text{Sn}\cdot\text{W}(\text{CO})_5\text{-SnL}^1$ (**4**)

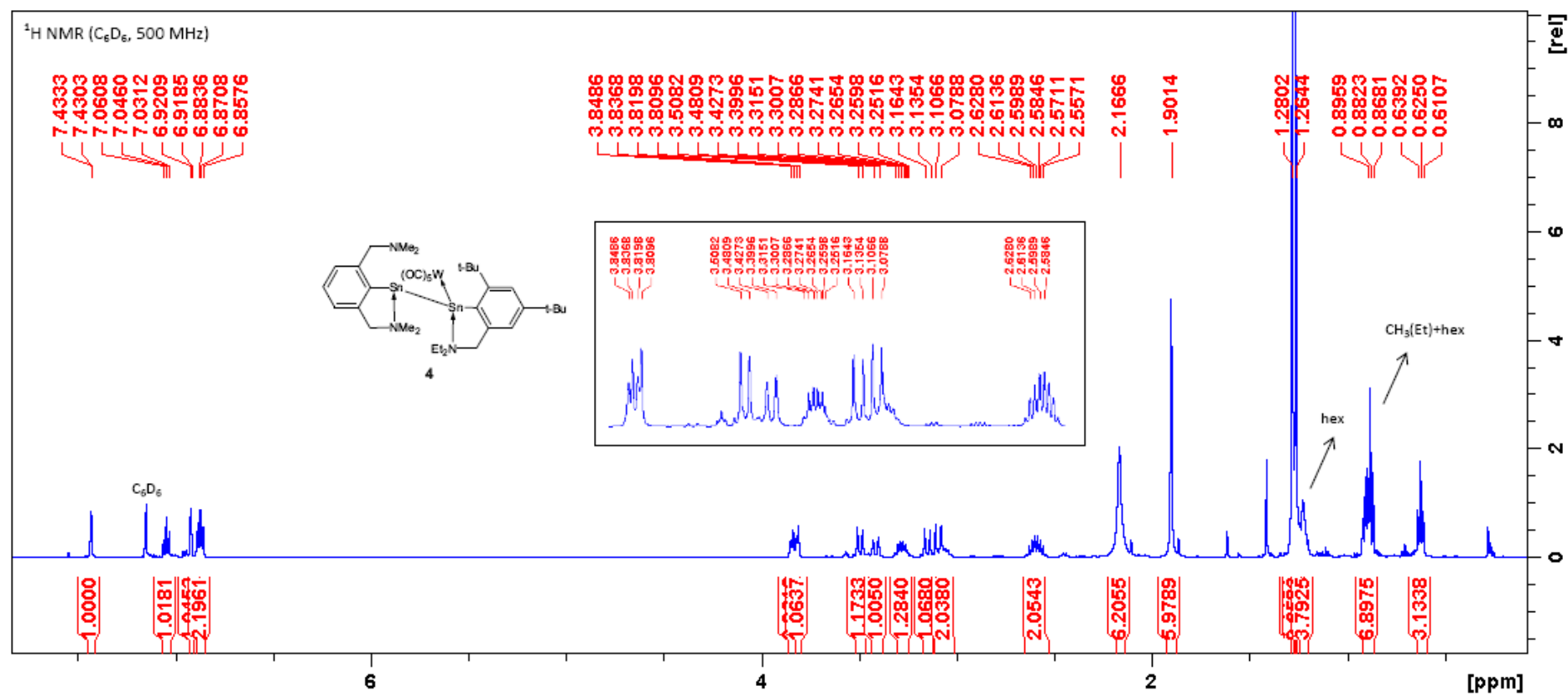


Figure S11. $^{13}\text{C}\{^1\text{H}\}$ APT NMR (C_6D_6 , 125 MHz) of $\text{L}^2\text{Sn}\cdot\text{W}(\text{CO})_5\text{-SnL}^1$ (**4**)

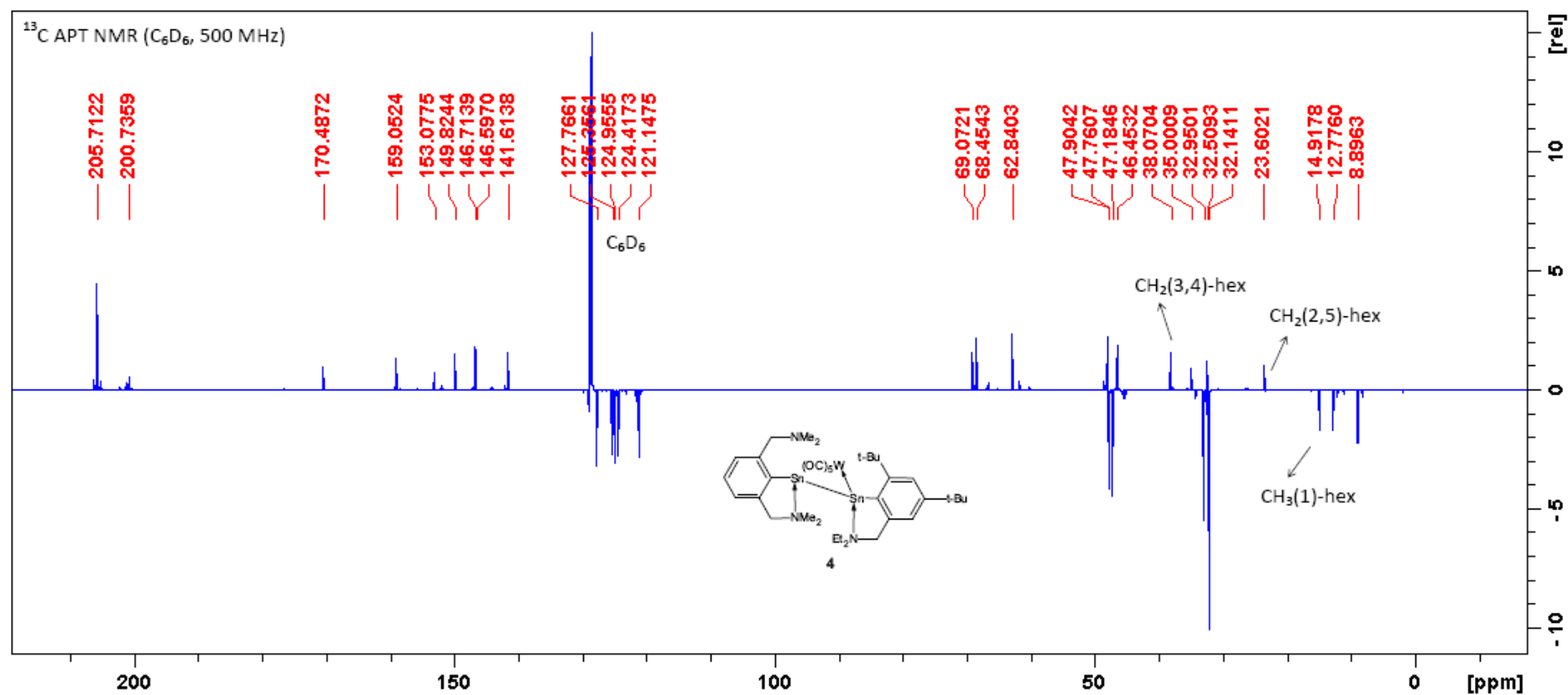


Figure S12. $^{119}\text{Sn}\{^1\text{H}\}$ NMR (C_6D_6 , 186 MHz) of $\text{L}^2\text{Sn}\cdot\text{W}(\text{CO})_5\text{-SnL}^1$ (**4**)

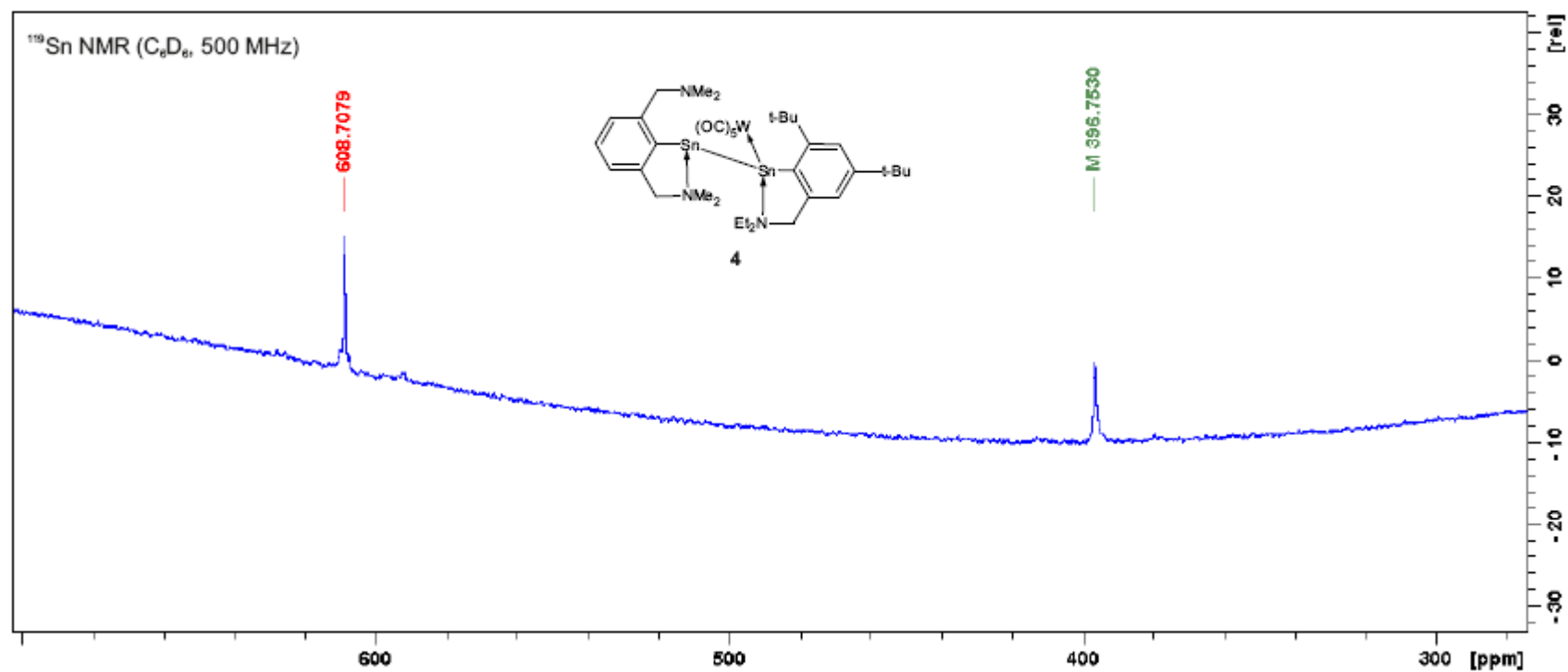
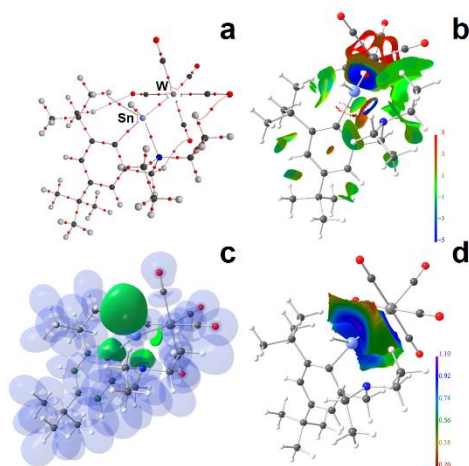


Figure S13. RSBI analysis of **2**. (a) AIM bond paths motif, (b) NCI *iso*-surface at $s(r) = 0.5$, (c) ELI-D localization domain representation at *iso*-value of 1.2, (d) ELI-D distribution mapped on the Sn–W ELI-D basin.



References

- (1) a) Jastrzebski, J.T.B.H.; van der Schaaf, P.A.; Boersma, J.; van Koten G.; Zoutberg, M.C.; Heijdenrijk, D. Synthesis and Characterization of {2,6-bis[(dimethylamino)methyl]phenyl}tin(II) Chloride and {2,6-bis[(dimethylamino)methyl]phenyl}(4-tolyl)tin(II), the First Example of a Mixed Diaryltin(II) Compound. *Organometallics* 1989, 8, 1373. b) Novák, M.; Bouška, M.; Dostál, L.; Růžička, A.; Hoffmann, A.; Herres-Pawlis, S.; Jambor, R. Less Is More: Three-Coordinate C,N-Chelated Distannynes and Digermynes. *Chem. Eur. J.* 2015, 21, 7820-7829.
- (2) Otwinowski, Z.; Minor, W. Processing of X-ray Diffraction Data Collected in Oscillation Mode. *Methods Enzymol.* **1997**, 276, 307-326.
- (3) Coppens, P. In: Ahmed, F.R.; Hall, S.R.; Huber, C.P. Editors, *Crystallographic Computing*, **1970**, 255-270, Copenhagen, Munksgaard.
- (4) Altomare, A.; Cascarano, G.; Giacovazzo, C.; Guagliardi, A. Early Finding of Preferred Orientation - a New Method. *J. Appl. Crystallogr.* **1994**, 27, 1045-1050.
- (5) Sheldrick, G.M. *SHELXT* – Integrated Space-Group and Crystal-Structure Determination. *Acta Cryst.* 2015, A71, 3-8.
- (6) Spek, A. L. *PLATON SQUEEZE*: A Tool for the Calculation of the Disordered Solvent Contribution to the Calculated Structure Factors. *Acta Cryst.* **2015**, C71, 9-18.
- (7) (a) Becke, A. D. A New Mixing of Hartree-Fock and Local-Density-Functional Theories. *J. Chem. Phys.* **1993**, 98, 5648-5652. (b) Perdew, J. P.; Chevary, J. A.; Vosko, S. H.; Jackson, K. A.; Pederson, M. R.; Singh, D. J.; Fiolhais, C. Atoms, Molecules, Solids, and Surfaces: Applications of the Generalized Gradient Approximation for Exchange and Correlation. *Phys. Rev. B* **1992**, 46, 6671-6687.

- (8) Frisch, M. J.; Trucks, G. W.; Schlegel, H. B.; Scuseria, G. E.; Robb, M. A.; Cheeseman, J. R.; Scalmani, G.; Barone, V.; Mennucci, B.; Petersson, G. A.; et al. *Gaussian09*, revision D.01; Gaussian, Inc.: Wallingford, CT, **2010**.
- (9) Wilson, A. J. C. *International Tables of Crystallography*; Kluwer Academic Publishers: Boston, **1992**; Vol. C.
- (10)(a) Figgen, D.; Peterson, K. A.; Dolg, M.; Stoll, H. Energy-consistent Pseudopotentials and Correlation Consistent Basis Sets for the 5d Elements Hf-Pt. *J. Chem. Phys.* **2009**, *130*, 164108. (b) Metz, B.; Stoll, H.; Dolg, M. Small-core Multiconfiguration-Dirac–Hartree–Fock-adjusted Pseudopotentials for Post-d Main Group Elements: Application to PbH and PbO. *J. Chem. Phys.* **2000**, *113*, 2563. (c) Peterson, K. A. Systematically Convergent Basis Sets with Relativistic Pseudopotentials. I. Correlation Consistent Basis Sets for the Post-d group 13–15 Elements. *J. Chem. Phys.* **2003**, *119*, 11099.
- (11) Bader, R. W. F. *Atoms in Molecules. A Quantum Theory*; Cambridge University Press: Oxford U.K., **1991**.
- (12) Biegler-König, F.; Schönbohm, J.; Bayles, D. A Program to Analyze and Visualize Atoms in Molecules. *J. Comput. Chem.* **2001**, *22*, 545-559.
- (13) Kohout, M. *DGRID-4.6* Radebeul, **2015**.
- (14) Kohout, M. A Measure of Electron Localizability. *Int. J. Quantum Chem.* **2004**, *97*, 651-658.
- (15) Johnson, E. R.; Keinan, S.; Mori-Sanchez, P.; Contreras-García, J.; Cohen, A. J.; Yang, W. Revealing Noncovalent Interactions. *J. Am. Chem. Soc.* **2010**, *132*, 6498-6506.
- (16) Contreras-García, J.; Johnson, E.; Keinan, S.; Chaudret, R.; Piquemal, J.-P.; Beratan, D.; Yang, W. NCIPLOT: A Program for Plotting Noncovalent Interaction Regions. *J. Chem. Theor. Comp.* **2011**, *7*, 625-632.
- (17) Hübschle, C. B.; Luger, P. MollIso – A Program for Colour-Mapped Iso-Surfaces. *J. Appl. Crystallogr.* **2006**, *39*, 901-904.